Bonding, Reactivity and Aromaticity in Some Beryllocene Derivatives*

Soma Duley, Puja Goyal, Santanab Giri, and Pratim Kumar Chattaraj[**]

Department of Chemistry and Center for Theoretical Studies, Indian Institute of Technology, Kharagpur 721302, India

Abstract. Geometries of $[X_3-M-Y_3]^{2-}$: X, M, Y = Be, Mg; $[Cp-M-Y_3]^-$: M, Y = Be, Mg and $[Cp-M-Cp]$; M = Be, Mg; $Cp^- = C_5H_5^-$ are optimized at the B3LYP/6-311+G(d) level of theory and the frequencies are also calculated at the same level of theory. Interesting bonding, reactivity and aromaticity trends emerge as one keeps on changing Cp^- units of beryllocene by the triangular aromatic dianions, X_3^{2-} (X = Be, Mg) as well as by replacing the central Be by Mg. Similar substitution of Cp^- by Al_4^{2-} and the additional change in the number of electrons yield all – metal complexes devoid of the original square planar Al_4^{2-} rings and with newly formed roughly rectangular aromatic rings. Atomic charges and Fukui functions lend additional insights into the local reactivity patterns of individual atomic centers.

Keywords: aromaticity, metal clusters, beryllocenes, conceptual DFT, NICS

INTRODUCTION

The synthesis and characterization of the structure of ferrocene[1,2] opened a new chapter in the field of organometallic chemistry. In general two cyclopentadienyl anion, $C_5H_5^-$ (Cp^-) rings or its pentamethyl derivatives (Cp^{*-}) form a sandwich like structure in these metallocenes where the metal ion stays in the middle. Aromaticity of the conjugated Cp^- system with 6π-electrons, above and below the metal ion provides stability towards this bis-metallocene $[Cp-M-Cp]$ complexes. In addition, for example in ferrocene, Fe^{2+} stays in the 2+ oxidation state and its 6 d-electrons together with 12 π-electrons from two Cp^- rings provide extra stability owing to the noble gas configuration with 18 electrons. Among the alkaline- earth sandwiches beryllocene is the smallest member. Unlike ferrocene, beryllocene is a slipped sandwich compound[3–5] where two Cp^- rings are neither parallel (eclipsed) nor antiparallel (staggered) to each other.

Synthesis of a variety of sandwich complexes by substituting Cp^- rings by other organic aromatic molecules[6] like benzene or cyclooctatetraene as well as by inorganic molecules[7] are reported. Ever since the discovery of all-metal aromatic systems[8] like Al_4^{2-} and all-metal antiaromatic systems[9] like Al_4^{4-} there has been a renewed interest in the study of metal clusters. Many of these systems exhibit both σ- and π- aromaticities and they possess a wide variety of structures including hexa-

gonal, pentagonal, tetragonal and triangular units, for example in[10–29] M_3^-: M = Al, Ga; X_3^-: X = Sc, Y, La; X_3^+: X = H, Li, Na, K, Cu; M_4^{2-}: M = Ge, In, Tl, Sb, Bi; M_4^{2+}: M = Sc, Te; Hg_4^{6-}; M_5^-: M = Sb, Bi; M_5^{6-}: M = Ge, Sn, Pb; Au_5Zn^+; Al_6^{2-}; MX_3: M = Li, Na, K, X = Sc, Y, La; XCl_3: X = H, Li, Na, K, Cu; *etc.* However, there exist metal clusters which are essentially π-aromatic,[30–33] *e.g.* Be_3^-, Mg_3^-, $NaMg_3^-$, Na_2Mg_3, M_3^{2-}: M = Zn, Cd, Hg, Be, Mg. In the present work we study the effect of substitution of Cp^- rings in beryllocene by some of the all metal aromatic rings. All of the reported structures may not correspond to global minima on the potential energy surface.

Stability, reactivity and aromaticity of a diverse class of chemical systems have been studied within a conceptual density functional framework.[34,35] Various global reactivity descriptors like electronegativity[36,37] (χ) and hardness[38–40] (η) and local reactivity descriptors like atomic charges[41] (Q_k) and the Fukui function[42] (f_k) have been used for this purpose. Associated electronic structure principles like the maximum hardness principle[43–45] (MHP) which states that, "There seems to be a rule of nature that molecules arrange themselves so as to be as hard as possible" provide additional insights. Due to an inverse relationship between the hardness and polarizability (α), a minimum polarizability principle[46,47] (MPP) has been proposed with the statement, "The natural direction of evolution of any system is towards a state of minimum polarizability." Here we analyze these

---

global and local reactivity descriptors apart from the standard aromaticity measure, the nucleus independent chemical shift[48] (NICS) in order to understand the bonding, reactivity and aromaticity patterns in some selected substituted beryllocene complexes. Section 2 provides the theoretical background of the present work whereas section 3 presents the numerical details. Results and discussion are presented in section 4 and finally section 5 contains some concluding remarks.

THEORETICAL BACKGROUND

For an *N*-electron system with total energy *E*, the electronegativity (χ)[36,37] and hardness (η)[38–40] are respectively defined as the following first-order and second order energy derivatives:

$$\chi = -\mu = -\left(\frac{\partial E}{\partial N}\right)_{v(\vec{r})} \tag{1}$$

and

$$\eta = \frac{1}{2}\left(\frac{\partial^2 E}{\partial N^2}\right)_{v(\vec{r})} \tag{2}$$

where μ and $v(\vec{r})$ are chemical and external potentials respectively.

A finite difference approximation to the above derivatives provides

$$\chi = \frac{I+A}{2} \tag{3}$$

and

$$\eta = \frac{I-A}{2} \tag{4}$$

where the ionization potential (*I*) and the electron affinity (*A*) are expressed in terms of the energy of an *N*-electron system, *E*(*N*), as

$$I \simeq E(N-1) - E(N) \tag{5}$$

and

$$A \simeq E(N) - E(N+1) \tag{6}$$

One of the most important local reactivity descriptors is the Fukui function,[42] $f(\vec{r})$ given by

$$f(\vec{r}) = \left(\frac{\partial \rho(\vec{r})}{\partial N}\right)_{v(\vec{r})} = \left(\frac{\delta \mu}{\delta v(\vec{r})}\right)_N \tag{7}$$

which means that it is a measure of the change in the electron density at a given point when electrons are

added to or removed from the system at constant $v(\vec{r})$ or equivalently it yields the change in the chemical potential when the external potential changes and the number of electrons remains conserved.

Condensation on individual atomic sites gives rise to:[49]

for nucleophilic attack

$$f_k^+ = q_k(N+1) - q_k(N) \tag{8a}$$

for electrophilic attack

$$f_k^- = q_k(N) - q_k(N-1) \tag{8b}$$

for radical attack

$$f_k^o = \left[q_k(N+1) - q_k(N-1)\right]/2 \tag{8c}$$

In Eqs. (8) q_k refers to the electronic population of atom k in a molecule.

The second order variation in energy as a response to an weak electric field ξ is described by electric dipole polarizability (α) as

$$\alpha_{i,j} = -\left(\frac{\partial^2 E}{\partial \xi_i \partial \xi_j}\right), \qquad i,j \equiv x,y,z \tag{9}$$

and the mean value of this quantity provides the isotropic dipole polarizability which is often measured experimentally, *i.e.*,

$$\alpha = \frac{1}{3}\left(\alpha_{xx} + \alpha_{yy} + \alpha_{zz}\right) \tag{10}$$

The absolute magnetic shielding is represented as the nucleus independent chemical shift (NICS)[48] which is designated as NICS(0) and NICS(1) when measured at the center of the ring in a molecule and 1 Å above the ring respectively.

NUMERICAL DETAILS

Molecular geometries of Be_3^{2-}, Mg_3^{2-}, $[X_3-M-Y_3]^{2-}$: X, M, Y = Be, Mg; $[Cp-M-Y_3]^-$: M, Y = Be, Mg and [Cp-M-Cp]; M = Be, Mg are optimized at the B3LYP/6-311+G(d) level of theory by using the Gaussian 03W suite of program.[50] The frequency calculation is performed at the same level of theory. The number of imaginary frequency is zero in all cases which confirms that the structures correspond to minima on the potential energy surface. The Gaussian 03 software[50] is used to
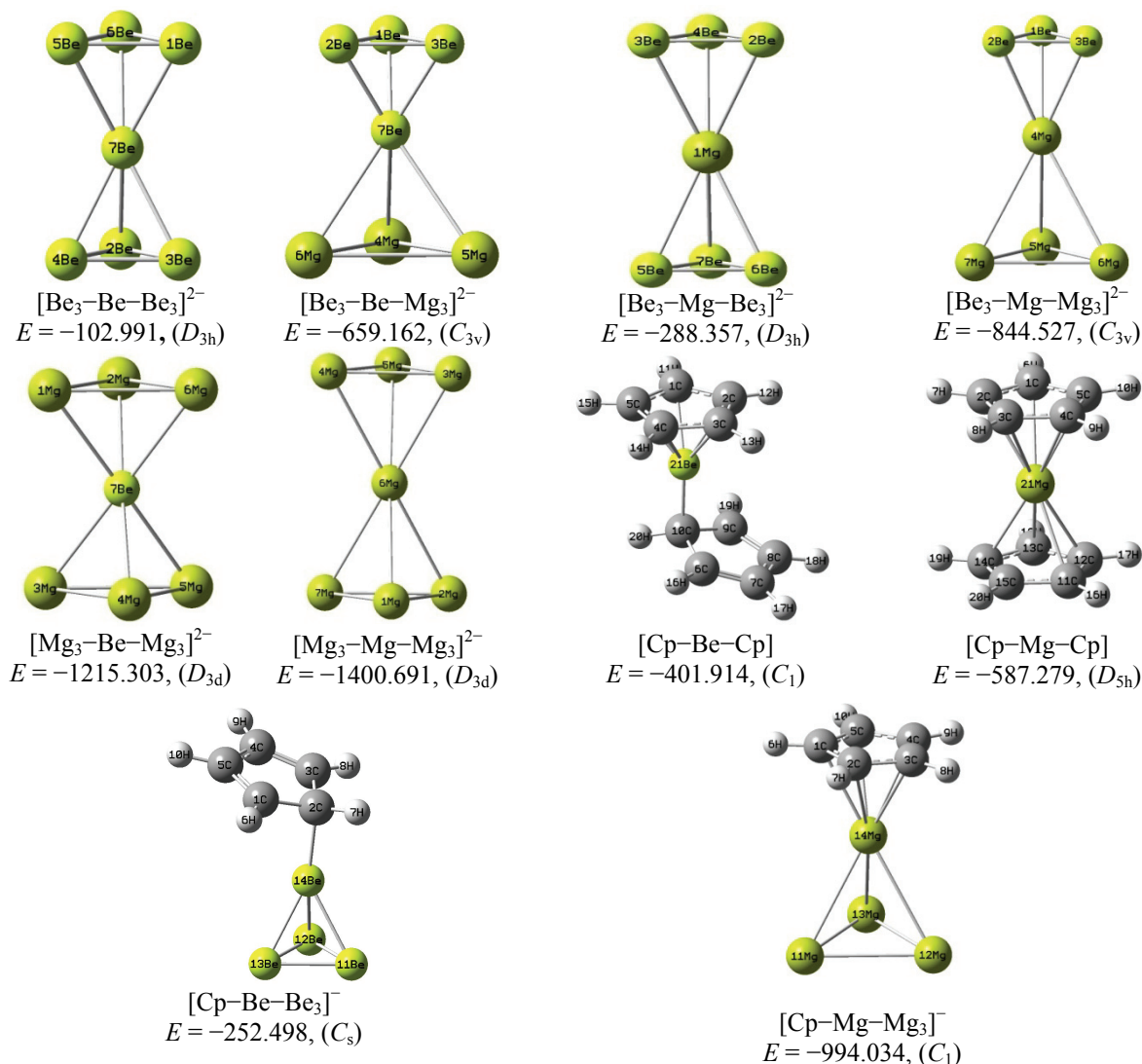
Figure 1. Optimized geometries (B3LYP/6-311+G(d)) of the $[Be_3-M-Be_3]^{2-}$, $[Mg_3-M-Mg_3]^{2-}$, $[Be_3-M-Mg_3]^{2-}$ and $[Cp-M-Cp]$ metallocenes (M = Be, Mg; *E* expressed in hartrees).

generate the molecular orbital pictures. First we substitute the Cp^- units of beryllocene by Be_3^{2-} and Mg_3^{2-} units both of which possess exclusively π-aromaticity. We also study the effect of substitution of the central Be^{2+} by Mg^{2+}. Finally we substitute the Cp^- units of beryllocene by Al_4^{2-} which exhibit both σ- and π-aromaticities.[51,52] The stability of saturated cyclic hydrocarbons with $(4n + 2)$ σ-electrons and no π-electron, *e.g.* cyclopropane, was explained in terms of σ-aromaticity which is also observed in the cases of systems like H_3^+ and Li_3^+. Often these systems exhibit large negative NICS values at the centre of the ring.[51] The last set of molecules is studied at the B3LYP/6-31G(d) level. After obtaining *I* and *A* using a ΔSCF technique, the hardness is calculated using Eq. (4). Polarizability is calculated as the linear response of the electron density

in the presence of a weak electric field and precisely as the related second-order variation in energy whereas NICS(0) and NICS(1) values are obtained by placing a dummy atom at the location where NICS value is calculated as the negative of the magnetic shielding. Mulliken population analysis (MPA) and natural population analysis (NPA) schemes are used in the calculation of atomic charges and Fukui functions.

RESULTS AND DISCUSSION

Optimized geometries of the selected beryllocenes and their derivatives are presented in Figure 1 and some important geometrical parameters (bond lengths and

Table 1. Point group, hardness (η / eV) and polarizability (α / eV) values of $[Be_3−M−Be_3]^{2−}$, $[Mg_3−M−Mg_3]^{2−}$, $[Be_3−M−Mg_3]^{2−}$ and [Cp−M−Cp] metallocenes (M = Be, Mg)

Metallocenes	Point Group	Hardness η / eV	Polarizability α / eV
[Cp−Be−Cp]	C_1	3.899	116.698
$[Cp−Be−Be_3]^−$	C_s	2.510	238.165
$[Be_3−Be−Be_3]^{2−}$	D_{3h}	1.506	711.320
$[Be_3−Be−Mg_3]^{2−}$	C_{3v}	1.232	974.745
$[Mg_3−Be−Mg_3]^{2−}$	D_{3d}	1.018	1654.977
[Cp−Mg−Cp]	D_{5h}	4.061	120.257
$[Cp−Mg−Mg_3]^−$	C_1	2.050	417.187
$[Be_3−Mg−Be_3]^{2−}$	D_{3h}	1.211	796.737
$[Be_3−Mg−Mg_3]^{2−}$	C_{3v}	1.121	1444.429
$[Mg_3−Mg−Mg_3]^{2−}$	D_{3d}	0.975	2358.555
$Be_3^{2−}$	D_{3h}	0.914	350.009
$Mg_3^{2−}$	D_{3h}	0.806	1128.921

Table 2. NICS(0) and NICS(1) values in different rings of $[Be_3−M−Be_3]^{2−}$, $[Mg_3−M−Mg_3]^{2−}$, $[Be_3−M−Mg_3]^{2−}$ and [Cp−M−Cp] metallocenes (M = Be, Mg)

Metallocenes	PG[a]	NICS(0) / ppm	NICS(1) / ppm
$[Be_3−Be−Be_3]^{2−}$	D_{3h}	−40.49 ($Be_3^{2−}$ unit, Upper)	−29.96 ($Be_3^{2−}$ unit, Upper)
		−40.49 ($Be_3^{2−}$ unit, Lower)	−14.79 ($Be_3^{2−}$ unit, Lower)
$[Be_3−Be−Mg_3]^{2−}$	C_{3v}	−36.28 ($Be_3^{2−}$ unit, Upper)	−18.67 ($Be_3^{2−}$ unit, Upper)
		−16.86 ($Mg_3^{2−}$ unit, Lower)	−16.41 ($Mg_3^{2−}$ unit, Lower)
$[Mg_3−Be−Mg_3]^{2−}$	D_{3d}	−18.58 ($Mg_3^{2−}$ unit, Upper)	−15.49 ($Mg_3^{2−}$ unit, Upper)
		−18.58 ($Mg_3^{2−}$ unit, Lower)	−8.69 ($Mg_3^{2−}$ unit, Lower)
[Cp−Be−Cp]	C_1	−17.47 (Cp$^−$ unit, Upper)	−27.34 (Cp$^−$ unit, Upper)
		−8.83 (Cp$^−$ unit, Lower)	−8.88 (Cp$^−$ unit, Lower)
$[Cp−Be−Be_3]^−$	C_s	−9.66 (Cp$^−$ unit, Upper)	−8.86 (Cp$^−$ unit, Upper)
		−39.43 ($Be_3^{2−}$ unit, Lower)	−22.43 ($Be_3^{2−}$ unit, Lower)
$[Be_3−Mg−Be_3]^{2−}$	D_{3h}	−42.50 ($Be_3^{2−}$ unit, Upper)	−21.96 ($Be_3^{2−}$ unit, Upper)
		−42.50 ($Be_3^{2−}$ unit, Lower)	−31.53 ($Be_3^{2−}$ unit, Lower)
$[Be_3−Mg−Mg_3]^{2−}$	C_{3v}	−40.59 ($Be_3^{2−}$ unit, Upper)	−32.46 ($Be_3^{2−}$ unit, Upper)
		−21.72 ($Mg_3^{2−}$ unit, Lower)	−16.94 ($Mg_3^{2−}$ unit, Lower)
$[Mg_3−Mg−Mg_3]^{2−}$	D_{3d}	−22.84 ($Mg_3^{2−}$ unit, Upper)	−16.46 ($Mg_3^{2−}$ unit, Upper)
		−22.84 ($Mg_3^{2−}$ unit, Lower)	−18.51 ($Mg_3^{2−}$ unit, Lower)
[Cp−Mg−Cp]	D_{5h}	−10.43 (Cp$^−$ unit, Upper)	−9.44 (Cp$^−$ unit, Upper)
		−10.43 (Cp$^−$ unit, Lower)	−11.56 (Cp$^−$ unit, Lower)
$[Cp−Mg−Mg_3]^−$	C_1	−15.92 (Cp$^−$ unit, Upper)	−11.06 (Cp$^−$ unit, Upper)
		−25.36 ($Mg_3^{2−}$ unit, Lower)	−18.36 ($Mg_3^{2−}$ unit, Lower)

[a] PG = Point group.

bond angles) are provided in Table SI (supporting information, Supplement). Starting with the beryllocene we substitute the Cp$^−$ rings by $Be_3^{2−}$ and $Mg_3^{2−}$ and also the central Be^{2+} by Mg^{2+}. Beryllocene possesses an (η^5 / η^5)-type slipped sandwich structure. Similar slipped structure persists when one Cp$^−$ is changed by a $Be_3^{2−}$ unit. However, substitution of both Cp$^−$ units by $Be_3^{2−}$

units provides a more symmetric (D_{3h}) sandwich structure. Symmetry gets slightly reduced by inserting one $Mg_3^{2−}$ unit in the place of a $Be_3^{2−}$ unit and it improves when both the $Be_3^{2−}$ units are replaced by $Mg_3^{2−}$ units. On the other hand the substitution of the central Be^{2+} by Mg^{2+} yields magnesocene with standard (η^5 / η^1)-geometry (D_{5h}). Further substitution of one or both Cp$^−$ by

Table 3. Substitution reactions

No.	Substitution reactions					ΔH / kcal mol^{-1}
1	$[Mg_3-Be-Mg_3]^{2-}$	+	Be_3^{2-}	$\rightleftarrows$	$[Be_3-Be-Mg_3]^{2-}$ + Mg_3^{2-}	−43.1
2	$[Be_3-Be-Mg_3]^{2-}$	+	Be_3^{2}	$\rightleftarrows$	$[Be_3-Be-Be_3]^{2-}$ + Mg_3^{2-}	−25.2
3	$[Mg_3-Be-Mg_3]^{2-}$	+	$2\ Be_3^{2-}$	$\rightleftarrows$	$[Be_3-Be-Be_3]^{2-}$ + $2\ Mg_3^{2-}$	−68.3
4	$[Mg_3-Mg-Mg_3]^{2-}$	+	Be^{2+}	$\rightleftarrows$	$[Mg_3-Be-Mg_3]^{2-}$ + Mg^{2+}	−125.6
5	$[Mg_3-Mg-Mg_3]^{2-}$	+	Be_3^{2-}	$\rightleftarrows$	$[Be_3-Mg-Mg_3]^{2-}$ + Mg_3^{2-}	−29.0
6	$[Be_3-Mg-Mg_3]^{2-}$	+	Be_3^{2-}	$\rightleftarrows$	$[Be_3-Mg-Be_3]^{2-}$ + Mg_3^{2-}	−25.4
7	$[Mg_3-Mg-Mg_3]^{2-}$	+	$2\ Be_3^{2-}$	$\rightleftarrows$	$[Be_3-Mg-Be_3]^{2-}$ + $2\ Mg_3^{2-}$	−54.4
8	$[Be_3-Mg-Be_3]^{2-}$	+	Be^{2+}	$\rightleftarrows$	$[Be_3-Be-Be_3]^{2-}$ + Mg^{2+}	−139.5
9	$[Be_3-Mg-Mg_3]^{2-}$	+	Be^{2+}	$\rightleftarrows$	$[Be_3-Be-Mg_3]^{2-}$ + Mg^{2+}	−139.7
10	$[Cp-Mg-Cp]$	+	Be^{2+}	$\rightleftarrows$	$[Cp-Be-Cp]$ + Mg^{2+}	−139.1
11	$[Cp-Be-Cp]$	+	Be_3^{2-}	$\rightleftarrows$	$[Cp-Be-Be_3]^{-}$ + Cp^{-}	−96.9
12	$[Cp-Be-Be_3]^{-}$	+	Be_3^{2-}	$\rightleftarrows$	$[Be_3-Be-Be_3]^{2-}$ + Cp^{-}	−38.8
13	$[Cp-Be-Be_3]^{-}$	+	Mg_3^{2-}	$\rightleftarrows$	$[Be_3-Be-Mg_3]^{2-}$ + Cp^{-}	−13.6
14	$[Cp-Be-Cp]$	+	$2\ Be_3^{2-}$	$\rightleftarrows$	$[Be_3-Be-Be_3]^{2-}$ + $2\ Cp^{-}$	−135.7
15	$[Cp-Mg-Cp]$	+	Mg_3^{2-}	$\rightleftarrows$	$[Cp-Mg-Mg_3]^{-}$ + Cp^{-}	−71.8
16	$[Cp-Mg-Mg_3]^{-}$	+	Mg_3^{2-}	$\rightleftarrows$	$[Mg_3-Mg-Mg_3]^{2-}$ + Cp^{-}	−9.2
17	$[Cp-Mg-Mg_3]^{-}$	+	Be_3^{2-}	$\rightleftarrows$	$[Be_3-Mg-Mg_3]^{2-}$ + Cp^{-}	−38.2
18	$[Cp-Mg-Cp]$	+	$2\ Mg_3^{2-}$	$\rightleftarrows$	$[Mg_3-Mg-Mg_3]^{2-}$ + $2\ Cp^{-}$	−81.0
19	$[Cp-Mg-Cp]$	+	$2\ Be_3^{2-}$	$\rightleftarrows$	$[Be_3-Mg-Be_3]^{2-}$ + $2\ Cp^{-}$	−135.4
20	$[Cp-Be-Cp]$	+	$2\ Mg_3^{2-}$	$\rightleftarrows$	$[Mg_3-Be-Mg_3]^{2-}$ + $2\ Cp^{-}$	−67.5

Be_3^{2-} or Mg_3^{2-} provides in general a less symmetric complex (D_{5h} goes to C_1, C_{3v}, D_{3d} or D_{3h}).

Table 1 presents the hardness and polarizability values of the beryllocene derivatives. Inverse relationship between hardness and polarizability is observed for (Be_3^{2-}, Mg_3^{2-}) pair as well as in $[Cp-Be-Cp]$ and its derivatives produced by substituting one or both Cp^- by Be_3^{2-} / Mg_3^{2-} and separately in $[Cp-Mg-Cp]$ and its derivatives obtained in the similar fashion.

Associated NICS(0) and NICS(1) values for two different rings in various metallocenes and their derivatives are reported in Table 2. All the rings are aromatic. Asymmetry in NICS(1) values of symmetric metallocenes (except $[Cp-Be-Cp]$ with C_1 symmetry): $[X-M-X]^{n-}$ is due to the position of M. It is, however, verified that identical NICS(1) values are observed when measured 1 Å above the upper ring and 1 Å below the lower ring. The NICS(0) values in these cases behave as expected. In general the aromaticity order is: $Be_3^{2-} > Mg_3^{2-} > Cp^-$. It may, however, be noted that when the upper and lower rings are different one may expect four different NICS(1) values. All the associated reactions in the thermodynamically favorable (forward) direction are presented in Table 3.

It is important to note that the order of preference of various units to form sandwich complexes is also the same, *viz.*, $Be_3^{2-} > Mg_3^{2-} > Cp^-$.

Atomic charges (MPA and NPA) and the related condensed Fukui functions on various centers are provided in Table 4. There is a characteristic difference between the atomic charges in complexes with or without Cp^-. While the central metal atom contains a positive charge and hence a preferable site for an attack by an anion or a hard nucleophile in the former the reverse trend is expected in the case of the latter complexes.

Similar trend is observed when atomic charges are obtained using natural population analysis (NPA). The ring atoms are negatively charged except for the Be_3^{2-} unit(s) in $[Be_3-Be-Mg_3]^{2-}$ and $[Be_3-Be-Be_3]^{2-}$ and the Mg_3^{2-} units in $[Mg_3-Mg-Mg_3]^{2-}$ but for NPA all the ring atoms are negatively charged. Both electrophilic and nucleophilic attacks (MPA) for soft species would be favored in the central metal atom in most cases. However, for NPA the situation is just the reverse in many cases. The Fukui function is negative in more number of cases for MPA. Figure 2 depicts the important frontier orbitals of those complexes. In majority of the cases the HOMO is π-bonding type where as the LUMO is of antibonding nature. In order to check the effect of σ-aromaticity in addition to π-aromaticity in stabilizing these complexes we study the substitution of Cp^- units of beryllocene by Al_4^{2-}. Since Al_4^{2-} is aromatic and Al_4^{4-} is claimed to be antiaromatic we also increase the number of electrons in $[Al_4-Be-Al_4]^{2-}$ to see its effect on complexation.

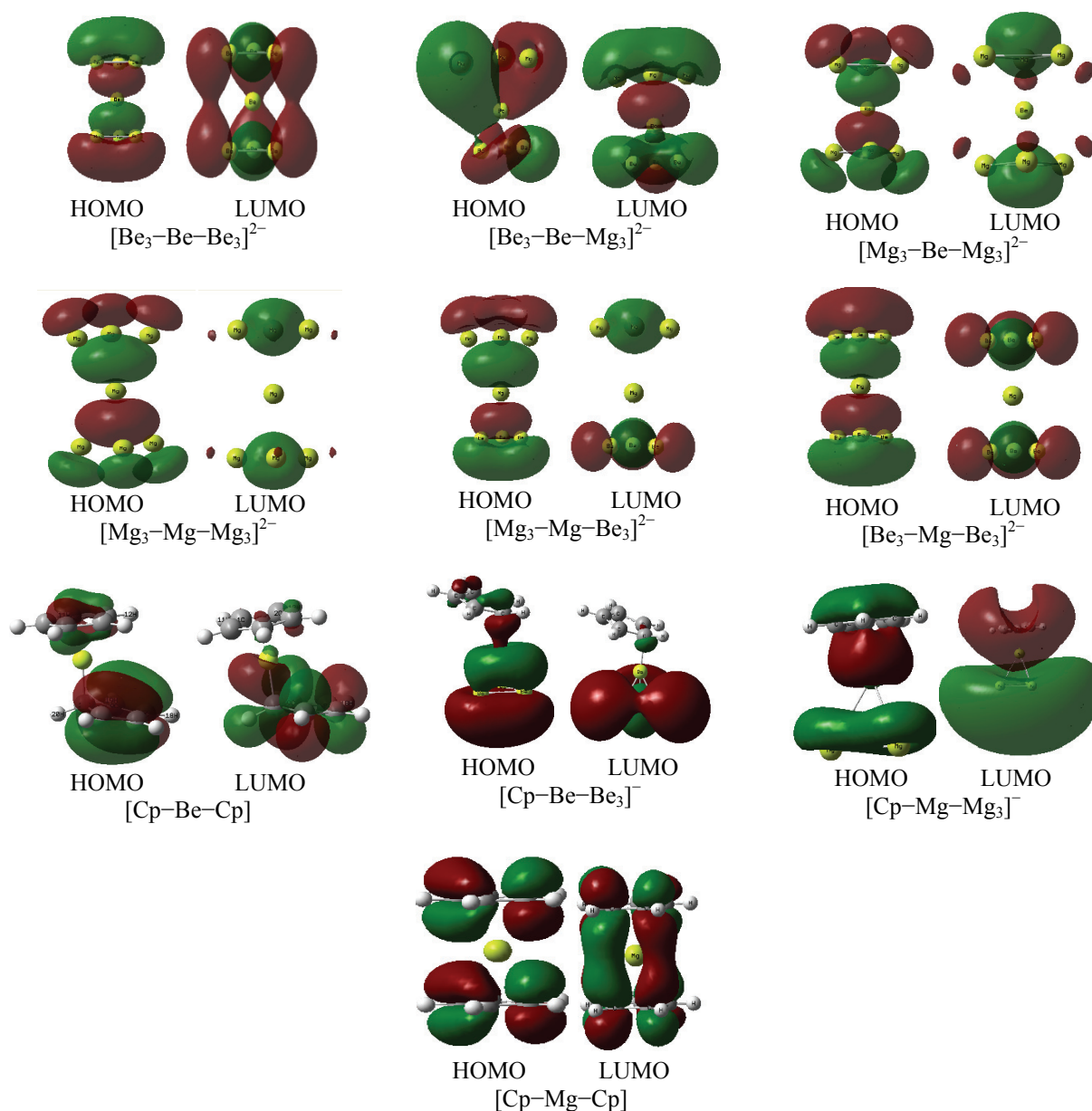Optimized structures of $[Al_4-Be-Al_4]^{n-}$: $n = 2$, 4, 5, 6 are presented in Figure 3 and some of their geome-

Table 4. Atomic charges (Q_k/e) and Fukui function values using MPA and NPA for the nucleophilic (f_k^+) and electrophilic (f_k^-) attacks at different sites of the $[Be_3-M-Be_3]^{2-}$, $[Mg_3-M-Mg_3]^{2-}$, $[Be_3-M-Mg_3]^{2-}$ and $[Cp-M-Cp]$ metallocenes (M = Be, Mg)

Metallocenes	Unit	Q_k/e MPA (NPA)	f_k^+ MPA (NPA)	f_k^- MPA (NPA)
$[Be_3-Be-Be_3]^{2-}$	Be_3^{2-}	1.093(−0.178), 1.087(−0.178), 1.109(−0.177)	0.736(0.191), 0.737(0.190), 0.695(0.190)	−1.221(0.149), −1.216(0.279), −1.232(0.101)
	Be_3^{2-}	1.106(−0.178), 1.090(−0.177), 1.085(−0.178)	0.800(0.190), 0.795(0.190), 0.838(0.190)	−1.234(0.278), −1.222(0.101), −1.217(0.149)
	Be	−8.569(−0.934)	−3.602(−0.142)	8.342(−0.057)
$[Be_3-Be-Mg_3]^{2-}$	Be_3^{2-}	2.132(−0.225), 2.116(−0.225), 2.117(−0.226)	−4.546(0.084), −4.473(0.083), −4.438(0.082)	−1.807(0.097), −1.795(0.096), −1.793(0.098)
	Mg_3^{2-}	−0.434(−0.081), −0.434(−0.081), −0.434(−0.081)	0.097(0.290), −0.048(0.301), 0.023(0.296)	0.195(0.086), 0.197(0.086), 0.196(0.086)
	Be	−7.063(−1.080)	14.385(−0.135)	5.806(0.451)
$[Mg_3-Be-Mg_3]^{2-}$	Mg_3^{2-}	−0.030(−0.078), −0.036(−0.078), −0.026(−0.077)	0.550(0.231), −0.903(0.234), −0.588(0.102)	−0.032(0.087), −0.027(0.088), −0.036(0.086)
	Mg_3^{2-}	−0.031(−0.078), −0.023(−0.077), −0.038(−0.078)	−0.914(0.102), −0.590(0.230), 0.574(0.235)	−0.031(0.088), −0.038(0.086), −0.025(0.088)
	Be	−1.816(−1.534)	2.871(0.133)	1.189(0.477)
$[Be_3-Mg-Be_3]^{2-}$	Be_3^{2-}	−0.159(−0.276), −0.159(−0.277), −0.159(−0.276)	−0.647(0.142), −0.646(0.143), −0.645(0.142)	−0.012(0.107), −0.012(0.109), −0.012(0.107)
	Be_3^{2-}	−0.159(−0.276), −0.159(−0.276), −0.159(−0.276)	−0.646(0.143), −0.647(0.142), −0.645(0.142)	−0.012(0.109), −0.012(0.107), −0.012(0.107)
	Mg	−1.048(−0.342)	4.876(0.147)	1.071(0.354)
$[Be_3-Mg-Mg_3]^{2-}$	Be_3^{2-}	−0.092(−0.305), −0.090(−0.305), −0.092(−0.305)	−0.599(0.086), −0.914(0.089), −0.588(0.086)	−0.016(0.088), −0.014(0.091), −0.015(0.089)
	Mg_3^{2-}	−0.245(−0.159), −0.245(−0.159), −0.245(−0.159)	−1.583(0.323), −1.587(0.323), −1.145(0.283)	0.097(0.101), 0.098(0.102), 0.098(0.102)
	Mg	−0.989(−0.608)	7.415(−0.190)	0.752(0.428)

(cont.)

Table 4. (continued)

[Mg₃–Mg–Mg₃]²⁻	Mg₃²⁻	0.655(−0.136), 0.649(−0.137), 0.666(−0.136)	−2.329(0.254), −2.318(0.256), −2.340(0.255)	−0.735(0.072), −0.728(0.073), −0.744(0.072)
	Mg₃²⁻	0.655(−0.136), 0.661(−0.135), 0.648(−0.136)	−2.327(0.256), −2.343(0.254), −2.323(0.255)	−0.734(0.073), −0.741(0.071), −0.727(0.073)
	Mg	−5.935(−1.184)	14.98(−0.529)	5.409(0.566)
[Cp–Be–Cp]	Cp⁻	−0.378(−0.402), −0.210(−0.396), −0.241(−0.400), −0.387(−0.399), −0.277(−0.397)	−0.784(0.035), −0.040(0.034), 0.068(−0.058), −0.725(0.052), −0.518(0.061)	0.056(0.029),−0.010(0.001), −0.013(−0.004), 0.060(0.028), 0.026(0.010)
	Cp⁻	−0.299(−0.238), −0.331(−0.268), −0.308(−0.268), −0.329(−0.238), −0.594(−0.833)	−0.659(0.001), −0.064(0.012), −0.002(0.011), −0.711(0.001), 1.062(0.006)	0.164(0.25 3),0.057(0.090),0.061(0.090), 0.163(0.253),−0.078(−0.017)
	Be	1.211(1.619)	3.077(0.724)	−0.086(−0.009)
[Cp–Mg–Cp]	Cp⁻	−0.285(−0.402), −0.285(−0.402), −0.285(−0.402), −0.285(−0.402), −0.285(−0.402)	−0.115(0.013), −0.127(0.013), −0.129(0.013), −0.129(0.013), −0.127(0.013)	0.030(0.048), 0.062(0.048), 0.039(0.137), 0.039(−0.004), 0.062(0.137)
	Cp⁻	−0.285(−0.402), −0.285(−0.402), −0.285(−0.402), −0.285(−0.402), −0.285(−0.402)	−0.129(0.013), −0.127(0.013), −0.115(0.013), −0.127(0.013), −0.129(0.013)	0.039(−0.004), 0.062(0.137), 0.030(0.048), 0.062(0.048), 0.039(0.137)
	Mg	0.824(1.794)	1.991(0.850)	−0.099(−0.014)
[Cp–Be–Be₃]⁻	Cp⁻	−0.442(−0.268), −0.084(−0.839), −0.442(−0.258), −0.300(−0.295), −0.300(−0.269)	−0.250(−0.013), 0.820(−0.005), −0.250(−0.004), −0.127(0.005), −0.127(0.030)	0.048(0.006), −0.130(0.044), 0.049(−0.004), 0.023(0.042), 0.023(0.016)
	Be₃²⁻	−0.118(−0.117), −0.242(−0.087), −0.242(−0.088)	−2.667(0.334), 1.799(0.239), 1.796(0.239)	0.232(0.104), 0.240(0.131), 0.240(0.130)
	Be	0.274(0.226)	−0.066(0.148)	0.114(0.458)
[Cp–Mg–Mg₃]⁻	Cp⁻	−0.273(−0.402), −0.270(−0.402), −0.276(−0.398), −0.292(−0.398), −0.279(−0.397)	−0.022(−0.001), −0.021(−0.001), −0.026(0.000), −0.003(0.001), −0.024(0.001)	−0.027(0.004), −0.030(0.005), −0.016(0.002), −0.022(0.002), −0.016(0.002)
	Mg₃²⁻	−0.227(−0.065), −0.234(−0.063), −0.232(−0.062)	−0.022(0.288), −0.016(0.295), −0.078(0.302)	0.231(0.096), 0.224(0.091), 0.223(0.088)
	Mg	0.215(0.161)	1.172(0.101)	0.299(0.654)

HOMO   LUMO
$[Be_3-Be-Be_3]^{2-}$

HOMO   LUMO
$[Be_3-Be-Mg_3]^{2-}$

HOMO   LUMO
$[Mg_3-Be-Mg_3]^{2-}$

HOMO   LUMO
$[Mg_3-Mg-Mg_3]^{2-}$

HOMO   LUMO
$[Mg_3-Mg-Be_3]^{2-}$

HOMO   LUMO
$[Be_3-Mg-Be_3]^{2-}$

HOMO   LUMO
$[Cp-Be-Cp]$

HOMO   LUMO
$[Cp-Be-Be_3]^-$

HOMO   LUMO
$[Cp-Mg-Mg_3]^-$

HOMO   LUMO
$[Cp-Mg-Cp]$

Figure 2. Some important frontier molecular orbital pictures of $[Be_3-M-Be_3]^{2-}$, $[Mg_3-M-Mg_3]^{2-}$, $[Be_3-M-Mg_3]^{2-}$ and $[Cp-M-Cp]$ metallocenes (M = Be, Mg).

trical parameters are presented in Table S2 (supporting information, Supplement).

Since Al_4^{2-} is a square planar (D_{4h}) aromatic molecule we replace two Cp⁻ units of beryllocene by two Al_4^{2-} units to form $[Al_4-Be-Al_4]^{2-}$. Unlike the different complexes analyzed in the preceding paragraphs the square planar geometry of each Al_4^{2-} units breaks down. Two new nearly rectangular frame works (1465 and 2387) are formed. The 2387 rectangular plane is absent in $[Al_4-Be-Al_4]^{5-}$ and unlike others the Be atom in this system does not remain in the middle of the 1465 plane, rather it stays slightly above the plane. In $[Al_4-Be-$ $Al_4]^{2-}$ the opposite pairs of angles are respectively acute and obtuse (not rectangular). However, the Be atom stays in the middle of the nearly rectangular 2387 plane of $[Al_4-Be-Al_4]^{n-}$, n = 2, 4, 6.

Table 5 reports the hardness and polarizability values of these systems. The inverse behavior between hardness and polarizability is observed only in the cases of $[Al_4-Be-Al_4]^{n-}$, n = 4, 6 presumably due to the difference in structure in the other complexes as mentioned above.

The NICS(0) and NICS(1) values on the 1465 ring of these systems are reported in Table 6. Most of the

Table 5. Point group, hardness (η / eV) and polarizability (α / eV) values of $[Al_4-Be-Al_4]^{n-}$ metallocenes

Metallocenes	Point Group	Hardness η / eV	Polarizability α / eV
$[Al_4-Be-Al_4]^{2-}$	D_{3d}	1.964	465.819
$[Al_4-Be-Al_4]^{4-}$	D_{3d}	2.180	576.927
$[Al_4-Be-Al_4]^{5-}$	C_s	1.696	635.362
$[Al_4-Be-Al_4]^{6-}$	D_{2h}	1.811	698.812
Al_4^{2-}	D_{4h}	2.681	275.256

Table 6. NICS(0) and NICS(1) values on the ring 1465 of $[Al_4-Be-Al_4]^{n-}$ metallocenes

Metallocenes (PG)[a]	NICS(0) / ppm	NICS(1) / ppm
$[Al_4-Be-Al_4]^{2-}$ (D_{3d})	−74.81	−11.01
$[Al_4-Be-Al_4]^{4-}$ (D_{3d})	−103.99	−35.28
$[Al_4-Be-Al_4]^{5-}$ (C_s)	−25.08	−36.85
$[Al_4-Be-Al_4]^{6-}$ (D_{2h})	−101.37	−29.70
Al_4^{2-} (D_{4h})	−33.18	−27.06

[a] Point group.

Table 7. Addition/substitution reactions

No.	Addition/Substitution Reactions:					ΔH / kcal mol^{-1}
1	$2\ Al_4^{2-}$ + Be^{2+}	⇌	$[Al_4-Be-Al_4]^{2-}$			−785.1
2	$2\ Al_4^{2-}$ + Be	⇌	$[Al_4-Be-Al_4]^{4-}$			115.4
3	$2\ Al_4^{2-}$ + Be^-	⇌	$[Al_4-Be-Al_4]^{5-}$			346.0
4	$2\ Al_4^{2-}$ + Be^{2-}	⇌	$[Al_4-Be-Al_4]^{6-}$			497.1
5	$[Al_4-Be-Al_4]^{4-}$ + Be^{2+}	⇌	$[Al_4-Be-Al_4]^{2-}$	+	Be	−916.9
6	$[Al_4-Be-Al_4]^{5-}$ + Be^{2+}	⇌	$[Al_4-Be-Al_4]^{2-}$	+	Be^-	−1147.4
7	$[Al_4-Be-Al_4]^{6-}$ + Be^{2+}	⇌	$[Al_4-Be-Al_4]^{2-}$	+	Be^{2-}	−1298.6
8	$[Al_4-Be-Al_4]^{6-}$ + Be^-	⇌	$[Al_4-Be-Al_4]^{5-}$	+	Be^{2-}	−151.2
9	$[Al_4-Be-Al_4]^{6-}$ + Be	⇌	$[Al_4-Be-Al_4]^{4-}$	+	Be^{2-}	−381.7
10	$[Al_4-Be-Al_4]^{5-}$ + Be	⇌	$[Al_4-Be-Al_4]^{4-}$	+	Be^-	−230.5
11	$[Cp-Be-Cp]$ + $2\ Al_4^{2-}$	⇌	$[Al_4-Be-Al_4]^{2-}$	+	$2\ Cp^-$	−104.2

rings are more aromatic than Al_4^{2-}. Even when Cp^- units are replaced by the antiaromatic Al_4^{4-} rings, the 1465 ring (in $[Al_4-Be-Al_4]^{6-}$) still remains aromatic.

It is important to note that NICS values may not be adequate in explaining the aromaticity / antiaromaticity in this type of systems as was highlighted through the related ring current studies.[53] While energy values show Al_4^{4-} to be antiaromatic as dictated by its photoelectron spectrum[9] and electron localization function values,[54] the polarizability and hardness values suggest[55] its (singlet) overall aromaticity (it is σ-aromatic and π-antiaromatic) as is also shown by their NICS[56] and magnetic field induced current density values.[57] Reac-

tion enthalpies of the associated reactions (forward direction) are provided in Table 7.

While most of the addition reactions are endothermic the substitution reactions are exothermic in nature. A simple increase in the number of electrons exhibits a drastic change in the nature of the frontier molecular orbitals (Figure 4).

Atomic charges (MPA and NPA) and the Fukui functions are reported in Table 8. In most cases for both MPA and NPA the Be-center is apt for an attack by an anion or a hard nucleophile while Al-centers are appropriate for an attack by a cation or a hard electrophile.

Table 8. Atomic charges (Q_k / e) and Fukui function values using MPA and NPA for the nucleophilic (f_k^+) and electrophilic (f_k^-) attacks at different sites of [Al$_4$–Be–Al$_4$]$^{n-}$ metallocenes

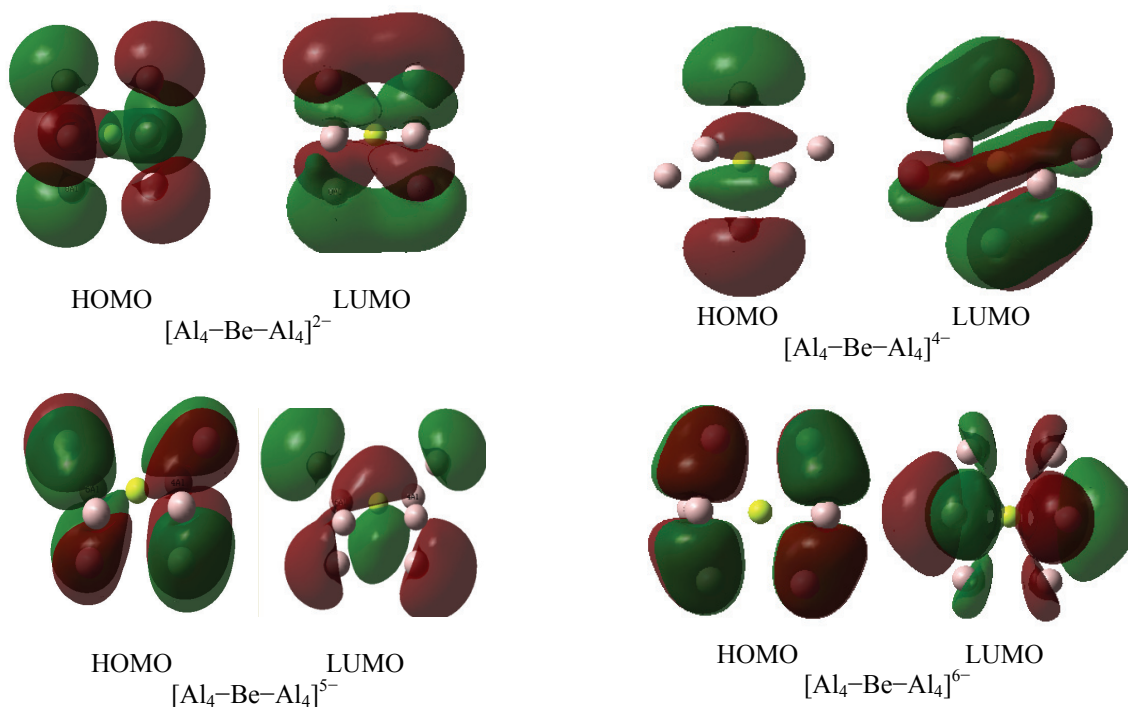| Metallocenes	Unit	Q_k / e MPA (NPA)	f_k^+ MPA (NPA)	f_k^- MPA (NPA)
[Al$_4$–Be–Al$_4$]$^{2-}$	Al	−0.145(−0.225), −0.279(−0.299), −0.279(−0.295), −0.279(−0.297)	0.193(0.162), 0.144(0.187), 0.135(0.161), 0.093(0.067)	0.137(0.103), 0.135(0.144), 0.134(0.144), 0.135(0.143)
	Al	−0.278(−0.296), −0.144(−0.222), −0.279(−0.300), −0.279(−0.297)	0.092(0.066), 0.190(0.159), 0.132(0.160), 0.141(0.182)	0.131(0.138), 0.137(0.102), 0.132(0.141), 0.132(0.142)
	Be^{2+}	−0.0380(0.231)	−0.119(−0.144)	−0.073(−0.055)
[Al$_4$–Be–Al$_4$]$^{4-}$	Al	−0.510(−0.597), −0.510(−0.597), −0.585(−0.506), −0.508(−0.598)	0.142(0.127), 0.155(0.090), 0.154(0.194), 0.126(0.155)	0.130(0.077), 0.133(0.080), 0.198(0.316), 0.137(0.083)
	Al	−0.511(−0.597), −0.509(−0.598), −0.590(−0.508), −0.511(−0.598)	0.126(0.156), 0.139(0.125), 0.157(0.196), 0.154(0.088)	0.131(0.076), 0.136(0.083), 0.202(0.319), 0.132(0.08)
	Be	0.234(0.598)	−0.150(−0.131)	−0.199(−0.115)
[Al$_4$–Be–Al$_4$]$^{5-}$	Al	−0.639(−0.784), −0.818(−0.709), −0.669(−0.655), −0.641(−0.784)	0.124(0.142), 0.214(0.142), 0.130(0.147), 0.124(0.142)	0.126(0.139), 0.216(0.158), 0.132(0.150), 0.126(0.140)
	Al	−0.625(−0.781), −0.626(−0.782), −0.832(−0.701), −0.632(−0.678)	0.093(0.108), 0.094(0.180), 0.233(0.203), 0.152(0.110)	0.099(0.111), 0.099(0.111), 0.238(0.204), 0.142(0.118)
	Be$^-$	0.483(0.875)	−0.165(−0.103)	−0.178(−0.130)
[Al$_4$–Be–Al$_4$]$^{6-}$	Al	−0.719(−0.940), −0.913(−0.798), −0.951(−0.814), −0.719(−0.939)	0.111(0.070), 0.172(0.180), 0.183(0.211), 0.111(0.070)	0.096(0.113), 0.189(0.158), 0.204(0.166), 0.096(0.113)
	Al	−0.720(−0.940), −0.718(−0.940), −0.914(−0.799), −0.952(−0.815)	0.111(0.069), 0.111(0.069), 0.172(0.181), 0.185(0.213)	0.097(0.114), 0.096(0.113), 0.190(0.159), 0.205(0.167)
	Be^{2-}	0.605(0.986)	−0.155(−0.063)	−0.174(−0.103)

$E = -1954.236 \ (D_{3d})$ $E = -1953.790 \ (D_{3d})$ $E = -1953.367 \ (C_s)$ $E = -1952.837 \ (D_{2h})$
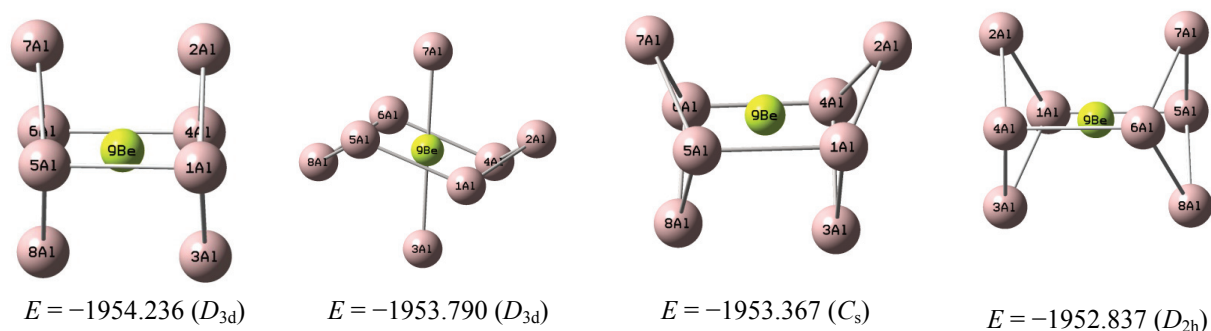
Figure 3. Optimized geometries (B3LYP/6-31G(d)) of $[Al_4-Be-Al_4]^{n-}$ metallocenes, $n = 2, 4, 5, 6$; E expressed in hartrees.

HOMO   LUMO
$[Al_4-Be-Al_4]^{2-}$

HOMO   LUMO
$[Al_4-Be-Al_4]^{4-}$

HOMO   LUMO
$[Al_4-Be-Al_4]^{5-}$

HOMO   LUMO
$[Al_4-Be-Al_4]^{6-}$

Figure 4. Some important frontier molecular orbital pictures of $[Al_4-Be-Al_4]^{n-}$ metallocenes, $n = 2, 4, 5, 6$.

As the overall charge increases, the reactivity of all the centers increases. The Al atoms are suitable for the attack by soft electrophiles and nucleophiles. The Fukui functions in the Be centers are all negative presumably due to the inadequacy of the MPA. The NPA-scheme also suffers from the same drawback.

CONCLUDING REMARKS

Bonding, reactivity and aromaticity patterns change drastically when the cyclopentadienyl anion rings and / or the central beryllium atom in beryllocene are changed. Substitution of Cp$^-$ rings by Be_3^{2-} and / or Mg_3^{2-} rings in general make the rings more aromatic and the associated replacement reactions are thermody-namically favorable. Substitution of Cp$^-$ rings by Al_4^{2-} cannot preserve the square planar nature of Al_4^{2-} although other aromatic rings are formed in course of their formation. Reactivity of various centers towards ions as well as hard /soft electro (nucleo) philes are delineated.

REFERENCES

1. T. J. Kealey and P. L. Pauson, *Nature* **168** (1951) 1039−1040.
2. S. Coriani, A. Haaland, T. Helgaker, and P. Jørgensen, *Chem. Phys. Chem.* **7** (2006) 245−249.
3. J. Demuynck and M. M. Rohmer, *Chem. Phys. Lett.* **54** (1978) 567−570.
4. C. Ning-Shih and L. Schaefer, *J. Am. Chem. Soc.* **100** (1978) 2604−2607.
5. A. Almenningen, A. Haaland, and J. Lusztyk, *J. Organomet. Chem.* **170** (1979) 271−284.
6. D. Seyferth, *Organometallics* **21** (2002) 2800−2820.
7. J. M. Mercero and J. M. Ugalde, *J. Am. Chem. Soc.* **126** (2004) 3380−3381.
8. X. Li, A.E. Kuznetsov, H.-F. Zhang, A. I. Boldyrev, and L. S. Wang, *Science* **291** (2001) 859−861
9. A. Kuznetsov, K. Birch, A. I. Boldyrev, X. Li, H. Zhai, and L. S. Wang, *Science* **300** (2003) 622−625.
10. K. K. Baeck and R. J. Bartlett, *J. Chem. Phys.* **109** (1998) 1334−1342.
11. A. E. Kuznetsov and A. I. Boldyrev, *Struct. Chem.* **13** (2002) 141−148.
12. L.-m. Yang, Y.-h. Ding, and C.-c. Sun, *Chem. Phys. Chem.* **7** (2006) 2478−2482.
13. X. X. Chi and Y. Liu, *Int J. Quantum. Chem.* **107** (2007) 1886−1896.
14. L. Yong, S. D. Wu, and X. X. Chi, *Int. J. Quantum Chem.* **107** (2007) 722−728.
15. A. E. Kuznetsov, A. I. Boldyrev, X. Li, and L. S. Wang *J. Am. Chem. Soc.* **123** (2001) 8825−8831.
16. B. Twamley and P. P. Power, *Angew. Chem., Int. Ed.* **39** (2000) 3500−3503.
17. A. Cisar and J. D. Corbett, *Inorg. Chem.* **16** (1977) 2482−2487.
18. S. C. Critchlow and J. D. Corbett, *Inorg. Chem.* **23** (1984) 770−774.
19. J. Barr, R. J. Gillespie, R. Kapoor, and G. P. Pez, *J. Am. Chem. Soc.* **90** (1968) 6855−6856.
20. T. W. Couch, D. A. Lokken, and J. D. Corbett, *Inorg. Chem.* **11** (1972) 357−362.
21. J. W. Nielsen and N. C. Baenziger, *Acta Crystallogr.* **7** (1954) 277−282.
22. A. E. Kuznetsov, J. D. Corbett, L. S. Wang, and A. I. Boldyrev, *Angew. Chem., Int. Ed.* **40** (2001) 3369−3372.
23. M. Gausa, R. Kaschner, H. O. Lutz, G. Seifert, and K.-H. Meiwes-Broer, *Chem. Phys. Lett.* **230** (1994) 99−102.
24. M. Gausa, R. Kaschner, G. Seifert, J.-H. Faehrmann, H. O. Lutz, and K.-H. Meiwes-Broer, *J. Chem. Phys.* **104** (1996) 9719−9728.
25. H. J. Zhai, L. S. Wang, A. E. Kuznetsov, and A. I. Boldyrev, *J. Phys. Chem. A* **106** (2002) 5600−5606.
26. I. Todorov and S. C. Sevov, *Inorg. Chem.* **43** (2004) 6490−6494.
27. I. Todorov and S. C. Sevov, *Inorg. Chem.* **44** (2005) 5361−5369.
28. H. Tanaka, S. Neukermans, E. Janssens, R. E. Silverans, and P. Lievens, *J. Am. Chem. Soc.* **125** (2003) 2862−2863.
29. A. E. Kuznetsov, A. I. Boldyrev, H.-J. Zhai, X. Li, and L.-S. Wang, *J. Am. Chem. Soc.* **124** (2002) 11791−11801.
30. L. Yong and X. Chi, *THEOCHEM* **818** (2007) 93−99.
31. A. E. Kuznetsov and A. I. Boldyrev, *Chem. Phys. Lett.* **388** (2004) 452− 456.
32. A. Velazquez, I. Fernández, G. Frenking, and G. Merino, *Organometallics* **26** (2007) 4731−4736.
33. D. R. Roy and P. K. Chattaraj, *J. Phys. Chem. A* **112** (2008) 1612−1621; D. R. Roy, S. Duley, and P. K. Chattaraj, *Proc. Indian Natl. Acad. Sci., Part A* **74** (2008) 11−18; P. K. Chattaraj, D. R. Roy, and S. Duley, *Chem. Phys. Lett.* **460** (2008) 382−385.
34. R. G. Parr and W. Yang, *Density Functional Theory of Atoms and Molecules*, Oxford University Press, New York, 1989.
35. P. K. Chattaraj (Ed.), *Chemical Reactivity Theory: A Density Functional View*, Taylor & Francis/CRC Press, Florida, 2009; P. Geerlings, F. De Proft, and W. Langenaeker, *Chem. Rev.* **103** (2003) 1793−1874; P. K. Chattaraj and S. Giri, *Annu. Rep. Prog. Chem., Sect. C: Phys. Chem.* **105** (2009) 13−39.
36. K. D. Sen and C. K. Jorgenson (Eds.), *Structure and Bonding*, Vol. 66, *Electronegativity*, Springer, Berlin, 1987.
37. R. G. Parr, R. A. Donnelly, M. Levy, and W. E. Palke, *J. Chem. Phys*, **68** (1978) 3801−3807.
38. K. D. Sen and D. M. P. Mingos (Eds.), *Structure and Bonding*, Vol. 80, *Chemical Hardness*, Springer, Berlin, 1993.
39. R. G. Parr and R. G. Pearson, *J. Am. Chem. Soc.* **105** (1983) 7512−7516.
40. R. G. Pearson, *Chemical Hardness*: *Applications from Molecules to Solids*, Wiley-VCH, Weinheim, 1997
41. R. S. Mulliken, *J. Chem. Phys.* **23** (1955) 1833−1840.
42. R. G. Parr and W. Yang, *J. Am. Chem. Soc.* **106** (1984) 4049−4050.
43. R. G. Pearson, *J. Chem. Educ.* **64** (1987) 561−567.
44. R. G. Parr and P. K. Chattaraj, *J. Am. Chem. Soc.* **113** (1991) 1854−1855.
45. P. W. Ayers and R. G. Parr, *J. Am. Chem. Soc.* **122** (2000) 2010−2018.
46. P. K. Chattaraj and S. Sengupta, *J. Phys. Chem.* **100** (1996) 16126−16130.
47. T. K. Ghanty and S. K. Ghosh, *J. Phys. Chem.* **100** (1996) 12295−12298.
48. P. v. R. Schleyer, C. Maerker, A. Dransfeld, H. Jiao, and N. J. R.v.E. Hommes, *J. Am. Chem. Soc.* **118** (1996) 6317.
49. W. Yang and W. J. Mortier, *J. Am. Chem. Soc.* **108** (1986) 5708−5711.
50. Gaussian 03, Revision B.03, Gaussian, Inc., Pittsburgh, PA.
51. Z. Chen, C. S. Wannere, C. Corminboeuf, R. Puchta, and P. v. R. Schleyer, *Chem. Rev.* **105** (2005) 3842−3888.
52. A. I. Boldyrev and L. S. Wang, *Chem. Rev.* **105** (2005) 3716−3757.
53. E. Steiner and P. W. Fowler, *Int. J. Quantum Chem.* **60** (1996) 609−616.
54. J. C. Santos, J. Andres, A. Aizman, and P. Fuentealba, *J. Chem. Theory Comput.* **1** (2005) 83−86.
55. P. K. Chattaraj, D. R. Roy, M. Elango, and V. Subramanian, *J. Phys. Chem. A* **109** (2005) 9590−9597.
56. Z. Chen, C. Corminboeuf, T. Heine, J. Bohmann, and P. v. R. Schleyer, *J. Am. Chem. Soc.* **125** (2003) 13930−13931.
57. R. W. A. Havenith, P. W. Fowler, E. Steiner, S. Shetty, D. Kanhere, and S. Pal, *Phys. Chem. Chem. Phys.* **6** (2004) 285−288.

SAŽETAK

Vezanje, reaktivnost i aromatičnost nekih derivata berilocena

Soma Duley, Puja Goyal, Santanab Giri i Pratim Kumar Chattaraj

Department of Chemistry and Center for Theoretical Studies, Indian Institute of Technology, Kharagpur 721302, India

Geometrije $[X_3-M-Y_3]^{2-}$ za X, M, Y = Be, Mg; $[Cp-M-Y_3]^-$ za M, Y = Be, Mg i $[Cp-M-Cp]$ za M = Be, Mg; $Cp^- = C_5H_5^-$ optimirane su na B3LYP/6-311+G(d) nivou teorije, kao i izračunate frekvencije. Zanimljivi se trendovi u vezanju, reaktivnosti i aromatičnosti pojavljuju zamjenom Cp^- fragmenata berilocena sa trokutastim aromatičnm dianionima, X_3^{2-} (X = Be, Mg), kao i zamjenom središnjeg Be sa Mg. Slična supstitucija Cp^- sa Al_4^{2-} i dodatna promjena u broju elektrona dovode do posve–metalnih kompleksa koji nemaju originalne kvadratično planarne Al_4^{2-} prstenove i do novoformiranih, pravokutnih aromatskih prstenova. Atomski naboji i Fukuijeve funkcije pružaju dodatni uvid u lokalne reaktivnosti individualnih atomskih centara.